

Phase Separation in the Melt and Confined Crystallization as the Key to Well-Ordered Microphase Separated Donor-Acceptor Block Copolymers

Ruth H. Lohwasser,[#] Gaurav Gupta,[§] Peter Kohn,[§] Michael Sommer, Andreas S. Lang,[#] Thomas Thurn-Albrecht,^{§*} Mukundan Thelakkat^{#*}

Synthesis scheme and structural analysis of P3HT-*b*-PPerAc7

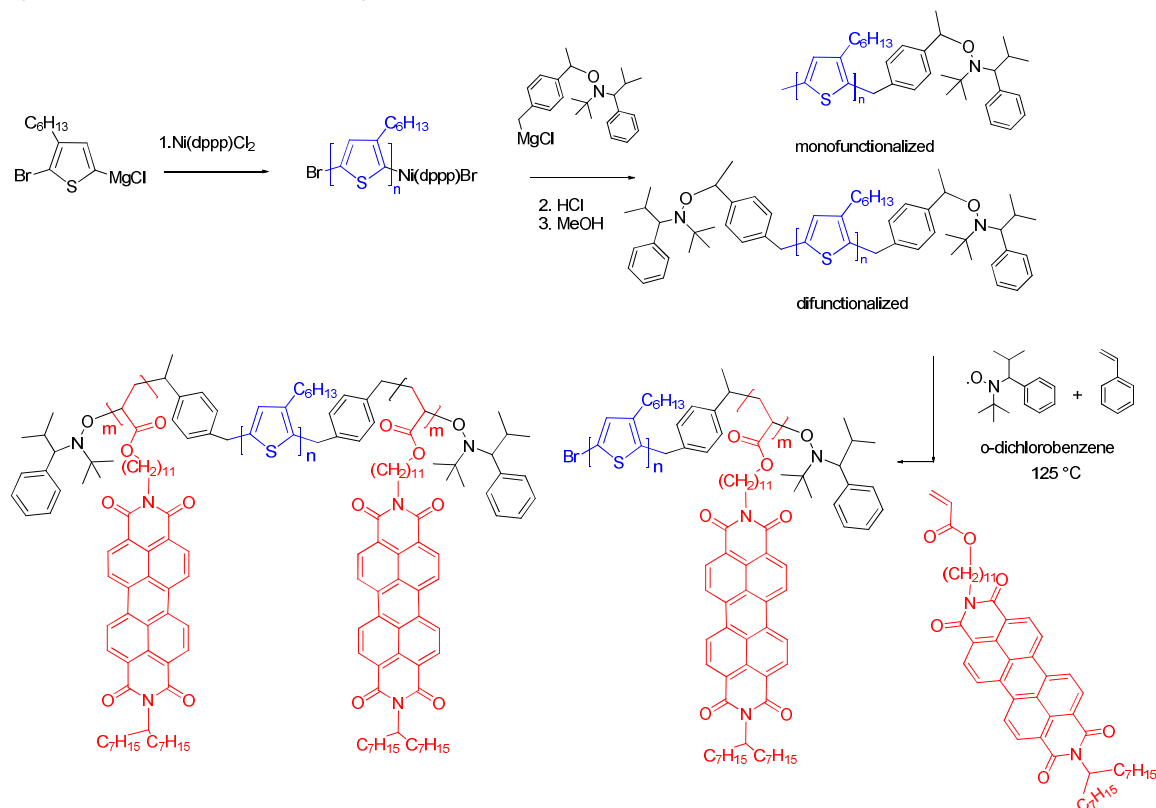


Figure SI 1: Reported synthetic scheme for P3HT-*b*-PPerAc7 using the in situ synthesis of the macroinitiator leading to mono- and difunctionalized macroinitiator and therefore di- and triblock copolymers.¹

X-Ray scattering and transmission electron microscopy of P3HT-*b*-PPerAc7

X-ray scattering on P3HT-*b*-PPerAc7 was performed at the beamline ID2 of the European Synchrotron Radiation Facility (ESRF) in Grenoble. The energy of the photons was 12.540 keV ($\lambda \sim 0.1$ nm). Aluminium discs with a central hole of 0.8 mm diameter served as sample holders which were mounted on a Linkam hotstage. Heat conducting paste was used to ensure good thermal contact. During the experiments samples were kept in nitrogen atmosphere to avoid degradation. We simultaneously used two detectors to cover a large range of scattering vectors q . The accessible q -ranges of the detectors had an overlap of approximately 1 nm^{-1} . P-bromo benzoic acid (PBBA) was used to calibrate the detectors. We estimated the resolution (minimum peak width due to the finite primary beam width of about $200 \mu\text{m}$) as $\Delta q \sim 0.02 \text{ nm}^{-1}$. The exposure time per pattern was 0.3 seconds. The scattering patterns were corrected by subtracting empty

cell measurements. Measurements were taken during cooling the sample from $T = 250^{\circ}\text{C}$ to $T = 90^{\circ}\text{C}$. At each temperature the sample was annealed for three minutes before recording the scattering pattern. The cooling rate between successive temperatures was 10 K/min. The sample preparation for TEM measurements was based on a similar thermal treatment as used for X-ray scattering. The samples were first heated above their melting temperature in aluminum pans as used in DSC measurements and then cooled to room temperatures. The heating and cooling rate was 10 K/min. Subsequently the samples were microtomed (thickness~ 80 nm) at room temperature and stained with vapors of RuO_4 for one hour. TEM measurements were performed with a JEOL 2010.

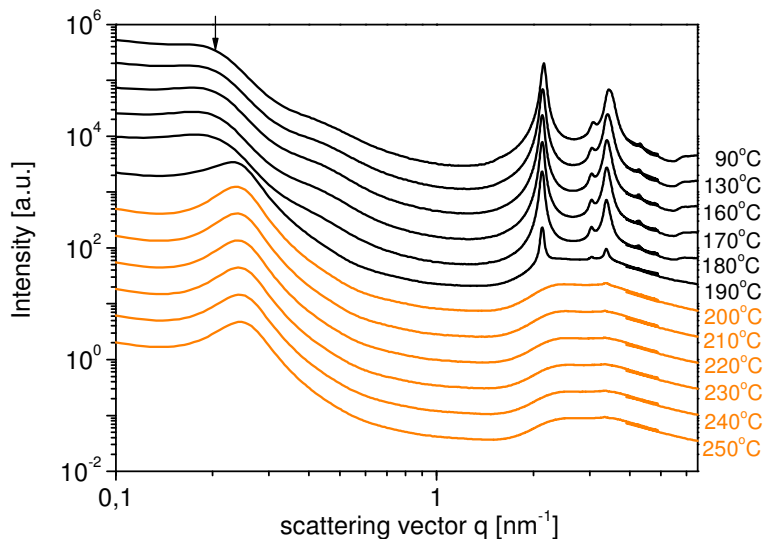


Figure SI 2: X-ray scattering patterns of P3HT-*b*-PPerAc 7 at the indicated temperatures during a stepwise cooling run.

Figure SI 2 shows the extended small angle X-ray patterns of P3HT-*b*-PPerAc 7 measured at different temperatures during stepwise cooling. While at high temperatures above 200°C only one broad peak around 0.25 nm^{-1} was observed, at about $T = 190^{\circ}\text{C}$ sharp Bragg-reflections developed at intermediate and large scattering vectors indicating ordering on length scales smaller than 1 nm. Again these reflections can be assigned to the well-known P3HT-lattice and the liquid crystalline structure formed in PPerAc. Simultaneously with the occurrence of molecular order the peak at small angles moves to the left and becomes broader. To answer the question whether the high temperature melt corresponds to a microphase separated state or a disordered melt, we analyzed the peak at $q \sim 0.25 \text{ nm}^{-1}$. On a qualitative level, there are obvious differences in comparison to the scattering pattern of the polymers P3HT-*b*-PPerAc 5 and 6. The peak is much broader ($\text{FWHM} \approx 0.074 \text{ nm}^{-1}$) and it has no higher orders. These observations suggest that it is caused by composition fluctuations as they occur in the disordered state and were first described by Leibler.² To check this assumption we analyzed the corresponding part of the scattering patterns in the high temperatures regime using the structure factor given by Leibler for the disordered phase.

$$I(q) = \frac{K}{F(q, f, R) - 2\chi N} + A \cdot \exp\left(\frac{-q^2}{B}\right)$$

Here N represents the degree of polymerization or number of segments, f the volume fraction, R the radius of gyration, and χ the Flory-Huggins interaction parameter. The function F in the denominator consists of several Debye-functions. An empirical background function was added with parameters A and B which were taken identical for all temperatures. We estimated the volume fraction of the PPerAc $f = 0.53$ from its mass fraction $f_m = 0.55$ and the crystallographic densities $\rho_{\text{PPerAc}} = 1.14 \text{ g cm}^{-3}$ and $\rho_{\text{P3HT}} = 1.06 \text{ g cm}^{-3}$ at $T = 90^{\circ}\text{C}$. These values were separately determined and are slightly different from the values obtained for P3HT-*b*-PPerAc 5 and 6. The result is shown in Figure SI 3. The model function describes the data well (a) and the resulting values for χN obtained at temperatures above 200°C are smaller than $(\chi N)_s = 10.56$, the value of the spinodal, at which within the mean field theory of Leibler, the transition to the ordered state would occur for the given volume fraction. This result confirms that for P3HT-*b*-PPEAc 7 ordering occurs from a disordered melt and is driven by crystallization. The shift of the peak in the scattering pattern reflects that crystallization is not confined in this material. Figure SI 4 shows a TEM image of the resulting nanostructure which is less ordered than the microphase structures in P3HT-*b*-PPEAc 5 and 6. 2

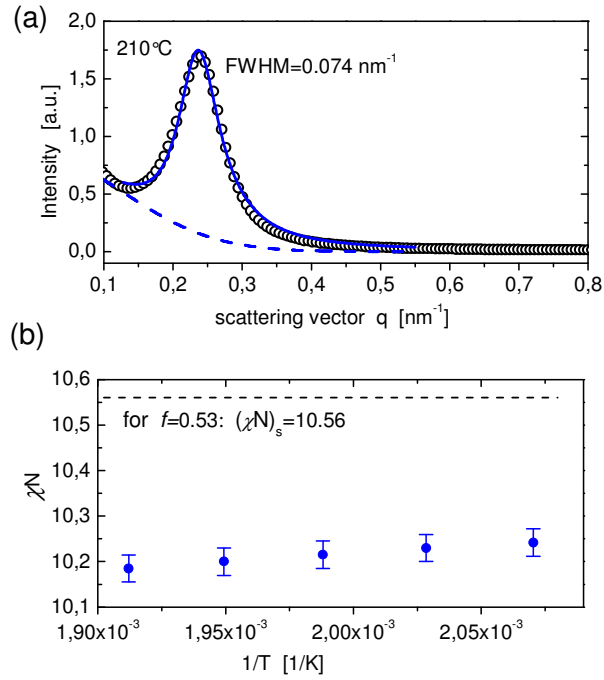


Figure SI 3: (a) Scattering intensity at $T=210^\circ\text{C}$ with model function (structure factor of a disordered block copolymer melt (solid line) and background intensity (dashed line). (b) The experimental values for χN (blue circles) in the molten state of the sample are smaller than the value $(\chi N)_s$, at which the transition to the ordered state occurs according to mean field theory.

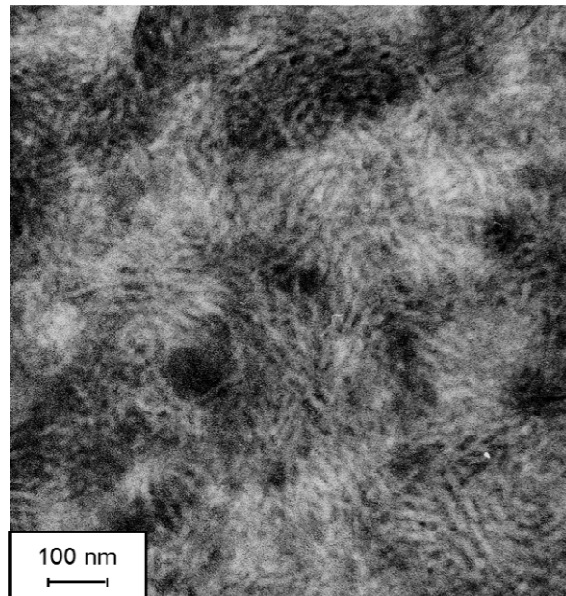


Figure SI 4: Transmission electron microscopy image of P3HT-*b*-PPerAcr 7.

Additional structural data for P3HT-*b*-PPerAc 5 and 6

Figure SI 5 shows the scattering patterns obtained for P3HT-*b*-PPerAc 5. The presentation and analysis is analogous to Figure 3 for the polymer 6 (see manuscript). In Figure SI 6, the scattering pattern for a) intermediate and b) high q range for P3HT-*b*-PPerAc 5 are shown and it is analogous to Figure 5 in the main text. Figure SI 7 shows an additional TEM image of P3HT-*b*-PPerAc 6 confirming cylindrical microdomains.

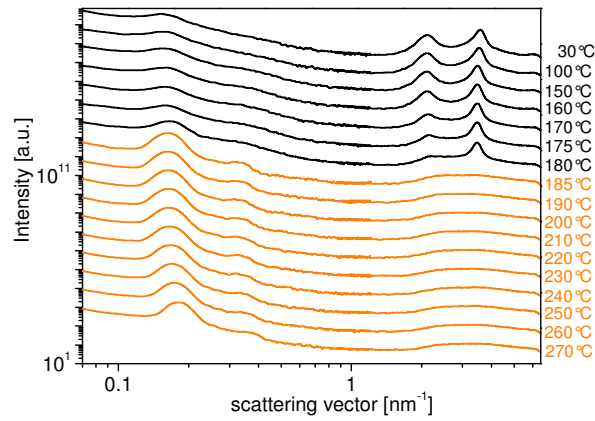


Figure SI 5: Scattering data at small and intermediate angles of P3HT-*b*-PPerAc 5 as recorded during cooling.

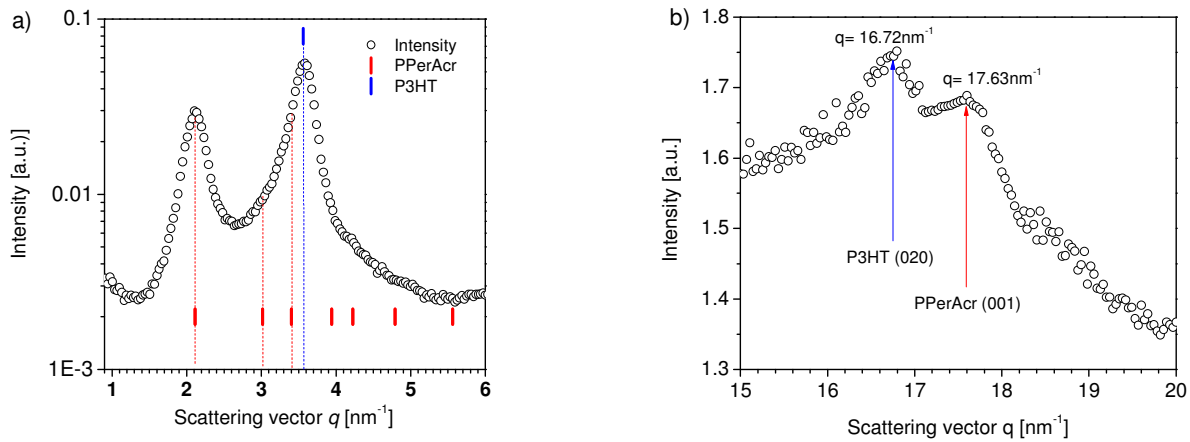


Figure SI 6: Scattering pattern for the block copolymer P3HT-*b*-PPerAc 5 at 30° for a) intermediate and b) high q range, showing the reflections for π - π stacking, with the reflections from P3HT marked in blue and the reflections from PPerAc marked in red.

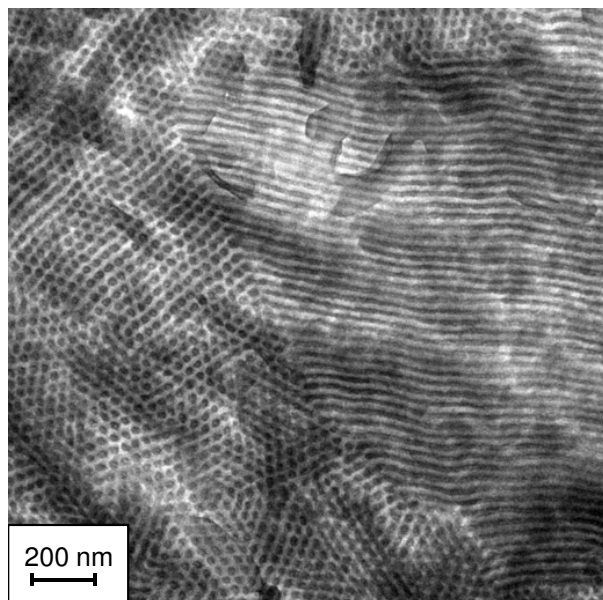


Figure SI 7: Transmission electron microscopy image of **6** in bulk showing a cylindrical morphology with lying and standing cylinders. The TEM samples were annealed for 1 h at 260°C and slowly cooled to room temperature with a cooling rate of 1°C/min. The P3HT phase was stained with RuO₄.

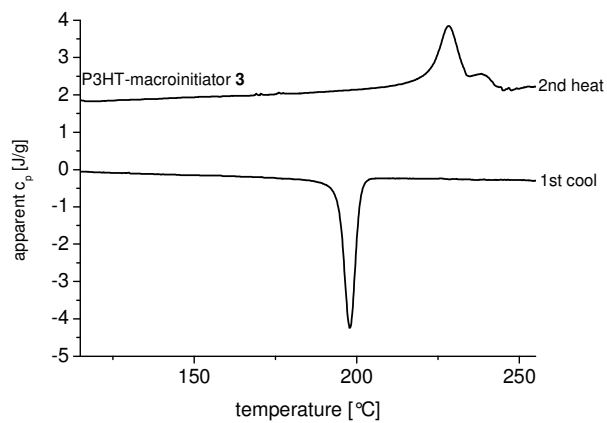


Figure SI 8: Differential scanning calorimetry curves of P3HT-macroinitiator **3**.

References

- (1) Sommer, M.; Hüttner, S.; Thelakkat, M. In *Advances in Polymer Science, Complex Macromolecular Systems II*, Müller, A. H. E and Schmidt, H. W., Eds.; Springer-Verlag: Berlin Heidelberg, 2010; p 123.
- (2) Leibler, L. *Macromolecules* **1980**, *13*, 1602-1617.